Nonlinear optical properties of graphene oxide in nanosecond and picosecond regimes

Zhibo Liu,[1] Yan Wang,[2] Xiaoliang Zhang,[1] Yanfei Xu,[2] Yongsheng Chen,[2,a)] and Jianguo Tian[1,b)]
[1]*Key Laboratory of Weak Light Nonlinear Photonics, Ministry of Education, and Teda Applied Physics School, Nankai University, Tianjin 300071, People's Republic of China*
[2]*Key Laboratory for Functional Polymer Materials and Centre for Nanoscale Science and Technology, and Institute of Polymer Chemistry, College of Chemistry, Nankai University, Tianjin 300071, People's Republic of China*

(Received 10 November 2008; accepted 18 December 2008; published online 12 January 2009)

The nonlinear optical properties of graphene oxide (GO) were investigated at 532 nm in nanosecond and picosecond regimes. Results show that two-photon absorption dominates nonlinear absorption process of GO in the case of picosecond pulses, while excited state nonlinearities play an important role in the case of nanosecond pulses. Additionally, we compared nonlinear optical properties of three different dimensional carbon-based materials (two-dimensional graphene, one-dimensional carbon nanotube, and zero-dimensional fullerene) in nanosecond and picosecond regimes, respectively. The nonlinear mechanism of GO is distinctly different from nonlinear scattering of carbon nanotube and excited state nonlinearity of fullerene. © *2009 American Institute of Physics*. [DOI: 10.1063/1.3068498]

Carbon exists in various allotropes: three-dimensional (3D) diamond, two-dimensional (2D) graphene, one-dimensional (1D) nanotube, and zero-dimensional (0D) fullerene. Scientists are familiar with the 3D, 1D, and 0D carbon nanostructures owing to their outstanding properties and great potential applications in many fields.[1,2] Graphene, as a very recent rising star in materials science with atomically thin 2D structure consisting of sp^2-hybridized carbon, exhibits remarkable electronic and mechanical properties.[3–6] Theoretically, the molecules of other carbon allotropic forms can be built from graphene. For example, 1D carbon nanotubes (CNTs) can be built by rolling up graphene with different layers and 0D fullerenes can be built by wrapping up from a single layer of graphene. It is known that perfect graphene itself does not exist and the solubility and/or processability come as the first issue for many perspective applications of graphene-based materials. So far, chemical functionalization of graphene has been focusing on improving its solubility/processability in both water and organic solvents[7,8] using different soluble groups. The presence of oxygen-containing groups in graphene oxide (GO) makes it strongly hydrophilic and water soluble.[8]

Both 1D CNT and 0D fullerene have been reported to have good optical nonlinear properties.[9–12] Single-walled CNTs (SWCNTs) and multiwalled CNT suspensions have been reported to have strong optical limiting effects in nanosecond regime.[12–14] However, fullerenes have large excited state absorption in nanosecond and picosecond regimes, which is a different nonlinear absorption (NLA) mechanism from CNT.[10] It is essential for applications of materials to make clear the mechanism of nonlinear optical (NLO) properties. Due to unique and large 2D π-electron conjugation systems of graphene, much like that in fullerene and CNTs, we expect that GO would exhibit good NLO properties. In this paper, we report the NLO properties of GO at 532 nm in nanosecond and picosecond regimes. Two-photon absorption dominates NLA process of GO in the case of picosecond pulse, which is distinctly different from CNT and fullerene.

GO was prepared by the modified Hummers method.[15] Atomic force microscopy (AFM) images confirmed that GO was comprised of isolated graphitic sheets. GO sample was prepared in the solution of DMF (*N*, *N*-Dimethylformamide). UV-visible (UV-vis) spectra were recorded on a VARIAN Cary 300 spectrophotometer using a quartz cell with a path length of 10 mm. Figure 1 shows the UV-vis absorption spectra of GO in DMF. GO shows a strong absorption band at 268 nm. The spectra are plotted in the wavelength range from 250 to 700 nm for DMF solution. Note that the bumpy plot in the short wavelength under ~270 nm is not reliable because of the strong absorption of solvent DMF and its unlikely complete compensation.[16] The inset in Fig. 1 is a typical tapping mode AFM image of GO sheets deposited on

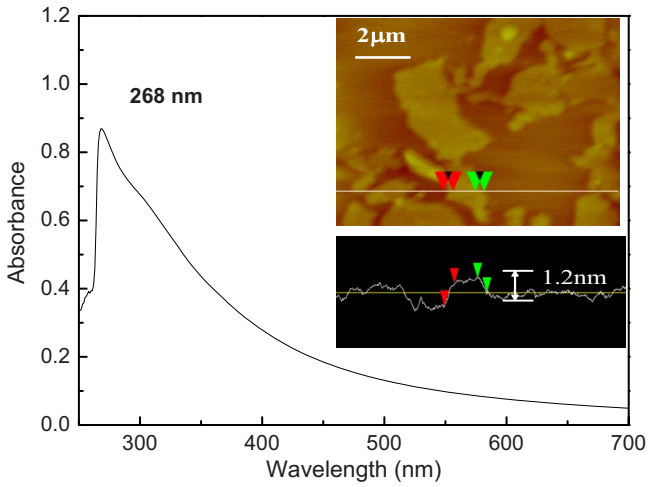

FIG. 1. (Color online) UV absorption of GO in DMF. The inset is an AFM image of GO sheets.

a)Electronic mail: yschen99@nankai.edu.cn.
b)Electronic mail: jjtian@nankai.edu.cn.

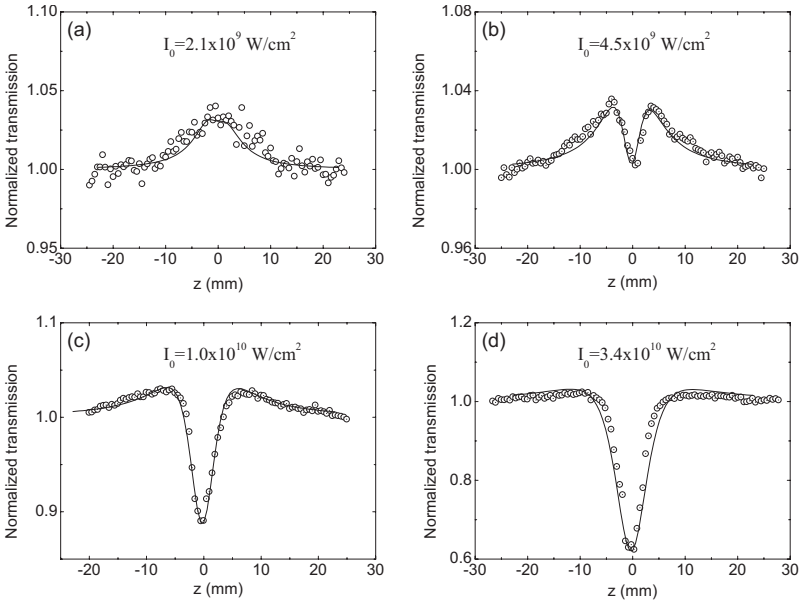

FIG. 2. Open aperture *Z*-scan curves of GO in DMF at different intensities. Solid lines represent theoretical fits obtained using Eqs. (1) and (2). I_0 is on-axis peak intensity at focus.

a mica substrate from a dispersion, and the height difference between arrows is ~1.2 nm, indicating an individual GO sheet. The average size of GO sheet is about 2 μm.

NLO properties of GO were measured by using *Z*-scan technique.[17] In *Z*-scan measurements, a *Q*-switched neodymium doped yttrium aluminum garnet (Nd:YAG) laser (Continuum Surelite-II) and a mode-locked Nd:YAG laser (Continuum model PY61) were used to generate 5 ns pulses and 35 ps pulses at 532 nm. The sample was filled in a 1-mm length quartz cell. The beam waist radius is about 20 μm. C_{60} was employed as a standard. No scattering signal was observed in the process of *Z*-scan measurements. Figure 2 gives open aperture picosecond *Z*-scan results of GO in DMF with concentration of 0.5 mg/ml at the input intensities of 2.1, 4.5, 10, and 34×10^9 W/cm^2, respectively. At the lowest input intensity of 2.1×10^9 W/cm^2, the normalized transmission curve in Fig. 2(a) shows a symmetrical peak with respect to the focus ($z=0$), indicating that saturable absorption (SA) in the sample dominates NLA mechanism. Remarkably, by increasing the input intensities to 4.5, 10, and 34×10^9 W/cm^2, as shown in Figs. 2(b)–2(d), a valley within the peak appears at the focus and becomes deeper increasingly, which implies that reverse saturable absorption (RSA) or two-photon absorption (TPA) appears following SA and finally a NLA transition occurs in GO.

Both SA and RSA originate from excited state absorption (ESA) process. When the absorption cross section of the excited state is smaller than that of the ground state, the transmission of the system will be increased when the system is highly excited. This process is called SA. ESA and TPA are the important processes leading to NLA behavior in organic materials. Under resonant and near resonant excitations, ESA is the dominant mechanism, whereas under nonresonant excitation TPA dominates the NLA behavior.[18] Under certain excitation conditions, both ESA and TPA may be operative simultaneously to lead to higher nonlinearities. From the abovementioned results, we can see two composite NLAs with opposite signs in the graphene solution at 532 nm. To interpret the flip of SA around the beam waist, we combine a SA coefficient and the TPA coefficient to yield the total absorption coefficient as[19]

$$\alpha(I) = \alpha_0 \frac{1}{1 + I/I_S} + \beta I, \tag{1}$$

where the first term describes SA and the second term describes positive NLA such as TPA. α_0 is the linear absorption coefficient, which is 789 m^{-1} for the graphene solution at 532 nm. I and I_S are laser radiation intensity and saturation intensity, respectively. β is TPA coefficient.

We theoretically fitted experimental results by solving the propagation equation of electric field envelope E:

$$\frac{1}{r}\frac{\partial}{\partial r}\left(r\frac{\partial E}{\partial r}\right) - 2ik\frac{\partial E}{\partial z} - ik\alpha E + \frac{2k^2}{n_0}n_2|E^2|E = 0, \tag{2}$$

where n_2 is nonlinear refractive index and k is wave vector. The numerical simulation of Eq. (2) was made by the Crank–Nicholson finite difference method. The best fit is obtained by using $I_s=2.1\times10^9$ W/cm^2 and $\beta=2.2\times10^{-9}$ cm/W. Theoretical simulations are in good agreement with the experimental results. This illustrates that the model we used is reasonable. The closed aperture *Z*-scan experiments showed that no obvious nonlinear refractive was observed.

In nanosecond regime, the origination of NLA will become more complicated due to participation of more excited state transitions.[20] Therefore, ESA will play a more important role in the case of nanosecond pulses. From nanosecond open aperture *Z*-scan results, we can see that TPA coefficient β changes as input intensity increases and $I_S=1.2\times10^8$ W/cm^2 was obtained. The value of β is larger about one order of magnitude than that in picosecond regime, respectively, which indicates that NLA of GO is enhanced greatly because of the contribution of ESA in nanosecond regime. To illustrate the difference in mechanism of NLA in nanosecond and picosecond regimes, we give NLA coefficient β as a function of input intensities for two different pulse widths in Figs. 3(a) and 3(b). With the increasing in input intensity, the value of β keeps almost the constant of 2.2×10^{-9} cm/W for picosecond pulses [Fig. 3(b)], while a clear enhancement of β can be observed from 2.9 to 5.6 $\times10^{-8}$ cm/W for nanosecond pulses [Fig. 3(a)]. The change

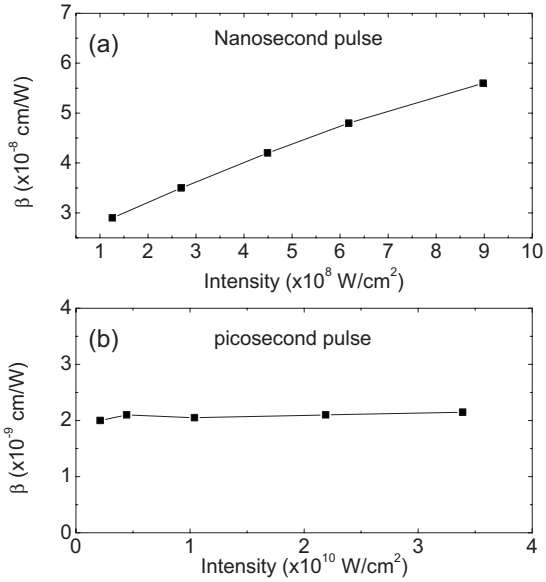

FIG. 3. NLA coefficient β as a function of input intensities for nanosecond and picosecond pulses.

in β with input intensity indicates that beside TPA, the contribution of ESA to NLA behavior of GO is also important in nanosecond regime.[20]

From the results mentioned above, GO in the DMF solution exhibits large TPA in picosecond regime and ESA in nanosecond regime. As the molecules of other carbon allotropic forms, fullerene and CNT have a different NLA process from graphene.[9,12] Although the mechanisms of NLA are different for these three carbon allotropic forms, to compare their optical nonlinearities qualitatively, we performed open aperture *Z*-scan measurements of GO, SWCNT in DMF, and C_{60} in toluene with same linear transmittance of 70% using picosecond and nanosecond pulses, as shown in Fig. 4. Since C_{60} has large singlet and triplet excited states

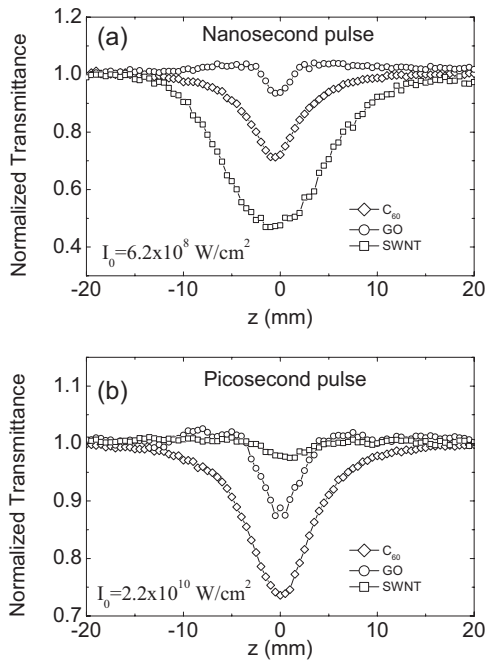

FIG. 4. Open aperture *Z*-scan curves of GO, SWCNT in DMF, and C_{60} in toluene for nanosecond pulses (a) and picosecond pulses (b).

absorption cross sections, it exhibits strong ESA for the two kinds of pulses. SWCNTs limiting action is strongest in the nanosecond time scale but is poorest in picosecond regime because strong nonlinear scattering happens in nanosecond regime. The 2D system exhibits much richer features of NLO response than 1D system. Therefore, the additional degrees of freedom associated with the 2D system may allow a finer modulation of the NLO response.[21]

In summary, we studied the NLA of GO in DMF using picosecond and nanosecond pulses. TPA and ESA were observed in picosecond and nanosecond regimes, respectively, and large TPA coefficient β was obtained. We compared the optical nonlinearities of three carbon nanomaterials, 0D fullerene, 1D CNT, and 2D graphene. Because graphene is lower cost and has different NLA mechanism from fullerene and CNT, we expect that graphene may bring a competitive entry into the realm of NLO materials for optoelectronic devices.

This work was supported by the NSFC (Grant Nos. 60708020, 10574075, and 20774047), Chinese National Key Basic Research Special Fund (Grant Nos. 2006CB921703 and 2006CB932702), and the Research Fund for the Doctoral Program of Higher Education of China (Grant No. 20070055045).

[1] P. M. Ajayan, Chem. Rev. (Washington, D.C.) **99**, 1787 (1999).
[2] N. Martin, L. Sanchez, B. Illescas, and I. Perez, Chem. Rev. (Washington, D.C.) **98**, 2527 (1998).
[3] D. Li and R. B. Kaner, Science **320**, 1170 (2008).
[4] D. A. Dikin, S. Stankovich, E. J. Zimney, R. D. Piner, G. H. B. Dommett, G. Evmenenko, S. T. Nguyen, and R. S. Ruoff, Nature (London) **448**, 457 (2007).
[5] J. S. Bunch, A. M. van der Zande, S. S. Verbridge, I. W. Frank, D. M. Tanenbaum, J. M. Parpia, H. G. Craighead, and P. L. Mceuen, Science **315**, 490 (2007).
[6] A. K. Geim and K. S. Novoselov, Nature Mater. **6**, 183 (2007).
[7] S. Niyogi, E. Bekyarova, M. E. Itkis, J. L. McWilliams, M. A. Hamon, and R. C. Haddon, J. Am. Chem. Soc. **128**, 7720 (2006).
[8] S. Stankovich, D. A. Dikin, G. H. B. Dommett, K. M. Kohlhaas, E. J. Zimney, E. A. Stach, R. D. Piner, S. T. Nguyen, and R. S. Ruoff, Nature (London) **442**, 282 (2006).
[9] L. W. Tutt and A. Kost, Nature (London) **356**, 225 (1992).
[10] D. G. McLean, R. L. Sutherland, M. C. Brant, D. M. Brandelik, P. A. Fleitz, and T. Pottenger, Opt. Lett. **18**, 858 (1993).
[11] Z. B. Liu, J. G. Tian, Z. Guo, D. M. Ren, F. Du, J. Y. Zheng, and Y. S. Chen, Adv. Mater. (Weinheim, Ger.) **20**, 511 (2008).
[12] L. Vivien, D. Riehl, F. Hache, and E. Anglaret, Physica B **323**, 233 (2002).
[13] P. Chen, X. Wu, X. Sun, J. Lin, W. Ji, and K. L. Tan, Phys. Rev. Lett. **82**, 2548 (1999).
[14] X. Sun, R. Q. Yu, G. Q. Xu, T. S. A. Hor, and W. Ji, Appl. Phys. Lett. **73**, 3632 (1998).
[15] H. A. Becerril, J. Mao, Z. F. Liu, R. M. Stoltenberg, Z. N. Bao, and Y. S. Chen, ACS Nano **2**, 463 (2008).
[16] J. I. Paredes, S. Villar-Rodil, A. Martinez-Alonso, and J. M. D. Tascon, Langmuir **24**, 10560 (2008).
[17] M. Sheikbahae, A. A. Said, T. H. Wei, D. J. Hagan, and E. W. Vanstryland, IEEE J. Quantum Electron. **26**, 760 (1990).
[18] P. P. Kiran, D. R. Reddy, A. K. Dharmadhikari, B. G. Maiya, G. R. Kumar, and D. N. Rao, Chem. Phys. Lett. **418**, 442 (2006).
[19] Y. Gao, X. Zhang, Y. Li, H. Liu, Y. Wang, Q. Chang, W. Jiao, and Y. Song, Opt. Commun. **251**, 429 (2005).
[20] R. L. Sutherland, *Handbook of Nonlinear Optics*, 2nd ed. (Dekker, New York, 2003).
[21] G. de la Torre, P. Vaquez, F. Agulló-Lopez, and T. Torres, Chem. Rev. (Washington, D.C.) **104**, 3723 (2004).